ASSOCIAZIONE NAZIONALE ITALIANA DI INGEGNERIA SISMICA
ANIDIS
Italian National Association of Earthquake Engineering

XVIII CONVEGNO ANIDIS
L'ingegneria sismica in Italia
ASCOLI PICENO 2019
15-19 Settembre

Flexure-shear interaction phenomena in seismic assessment of reinforced concrete frames

Angelo Pelle[a], Alessandro Rasulo[a], Davide Lavorato[b], Gabriele Fiorentino[b], Camillo Nuti[b], Bruno Briseghella[c]
a Dept. of Civil and Mechanical Engineering, Univ. of Cassino and Southern Lazio, Cassino, Italy
b Dept. of Architecture, Roma Tre University, Largo G. B. Marzi 10, 00153, Roma, Italy
c College of Civil Engineering of Fuzhou University, Fuzhou, China

Keywords: Seismic assessment, Shear strength, Opensees, Collapse Modes

ABSTRACT
Seismic assessment of reinforced concrete (RC) buildings under seismic loading requires the ability to model the effective non-linear response and to identify the relevant failure modes of the structure. Due to the lack of application of capacity design principles, existing RC structures can exhibit premature shear failures with a reduction of available strength and ductility. In particular, several researches have shown that the shear strength decrease with the increase of flexural damage after the development of plastic hinges and, in some cases, this can cause a premature and unexpected shear failure in the plastic branch with a consequent reduction of ductility. The scope of this paper is to study the flexural-shear interaction phenomena in order to understand their influence on the behaviour of the structures and to show how these phenomena can be implemented in a finite-element analysis. The analysis have been conducted with Opensees that has specific commands able to model the flexural-shear interaction phenomena. In the present research a specific model was developed, implementing some state-of-the-art simplified models aiming at capturing the complex interaction between shear and flexural damage mechanisms have been proposed and implemented in regulatory building codes and guidelines. Based on this model, a series of validation analysis have been performed, in order to verify the reliability of the formulation.

1 INTRODUCTION

Existing buildings in Italy are particularly vulnerable to seismic action. This is due to a concurrence of different factors such as the late adoption of modern design codes and the low rate of renovation of the building stock. In fact less than 23 % of Italian buildings have been built after 1980 (when a major revision of the seismic code was implemented as a consequence of the Irpinia earthquake) (Rasulo et al. 2015, Rasulo et al. 2016). It is a matter of fact that their vulnerability represent a serious social concern in term of life safety and of economic losses, as demonstrated by the consequences of some of the most recent moderate to strong Italian earthquakes (Molise 2002, L'Aquila 2009, Emilia Romagna 2012, Central Italy 2016) (Di Ludovico et al. 2017, Marino et al. 2019). It is therefore urgent to undertake retrofit or rebuilding measures for potentially non-conforming structures (Imperatore et al 2012, Lavorato et al. 2017, Imperatore et al. 2013, Forte et al. 2018, Lavorato et al. 2018a, Lavorato et al. 2018b, Lavorato et al. 2019).

Regarding reinforced concrete (RC) buildings, in particular, they have been generally conceived just to withstand the gravity loads (since most of national territory was, at the time of their construction, not recognized to be seismically prone) and designed according to older construction standards, based on the admissible stress method and without capacity design provisions. One of the common characteristic of their construction, that would be considered substandard according to the modern construction practice, is the presence of a low percentage of transversal reinforcement usually represented by poorly detailed and highly spaced stirrups.

According to the experimental evidence, structures with such a characteristic have a limited capacity to dissipate energy undergoing inelastic

deformation and in some cases can show a brittle response such as a shear failure. In fact, several researches and studies on shear strength have shown that the columns subjected to cyclic lateral loading may fail early, in shear, after the attainment of the flexural yielding, even in such a cases where the column was designed with a nominal shear capacity exceeding the shear force in equilibrium with bending (Zhou et al. 2014, Zhou et al. 2015, Calvi et al. 2000, Calvi et al. 2005).

Indeed the widening of flexural–shear cracks due to cyclic inelastic flexural deformations in the plastic-hinge region interfere with the concrete shear transfer mechanism relying on the aggregate interlock phenomena, with a consequent reduction of the sectional shear capacity, demonstrating that under cyclic loading the shear strength of columns can be heavily dependent on the inelastic deformations and that shear strength degrades with ductility more quickly than flexural strength. Thus, it is important, when assessing the seismic response of existing structures, that in the numerical model all the relevant phenomena that can influence the final performance of the structure are accounted for.

The aim of this paper is to propose an OpenSEES numerical model which can take into account the shear behavior other than the flexural one in order to investigate potential brittle failures.

2 OPENSEES MODEL

The numerical model adopted in this research to reproduce the seismic response of a RC element is based on a three-component approach, in which the following coexisting behavioural mechanisms are separately accounted for: flexure, bonding and shear. As schematically depicted in Figure 1 and 2, the lateral displacement of a column can, indeed, be represented as the sum of those three components. Flexure is by far the most relevant aspect in determining the seismic response of a column and it is also the most investigated one. The bonding is responsible for the extra displacement due to the slippage of the longitudinal reinforcing bars in the anchoring concrete. This phenomenon can be represented as a fixed-end rotation of the column, due to the strain penetration of steel bars anchored within the adjacent elements (the foundation for the columns at the base of the building or through the joints for

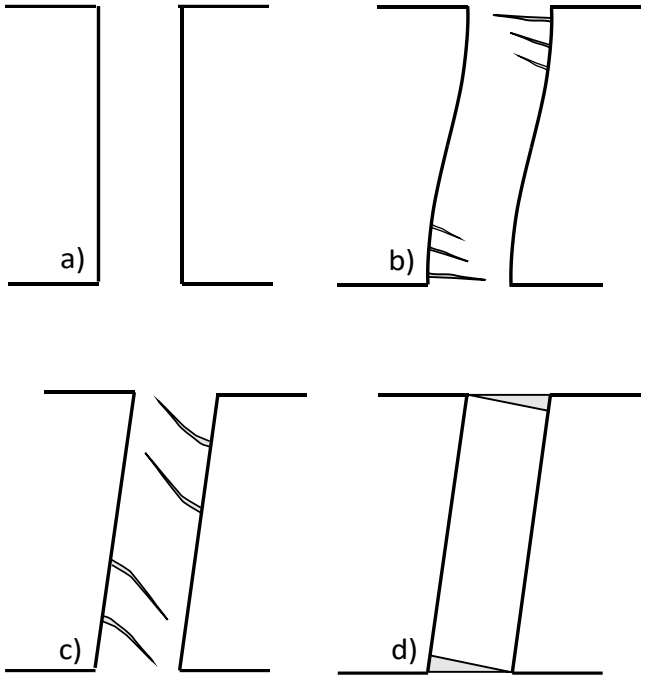

Figure 1. Components of horizontal displacement. a) original configuration; b) bending deformation; c) shear deformation and d) bonding deformation.

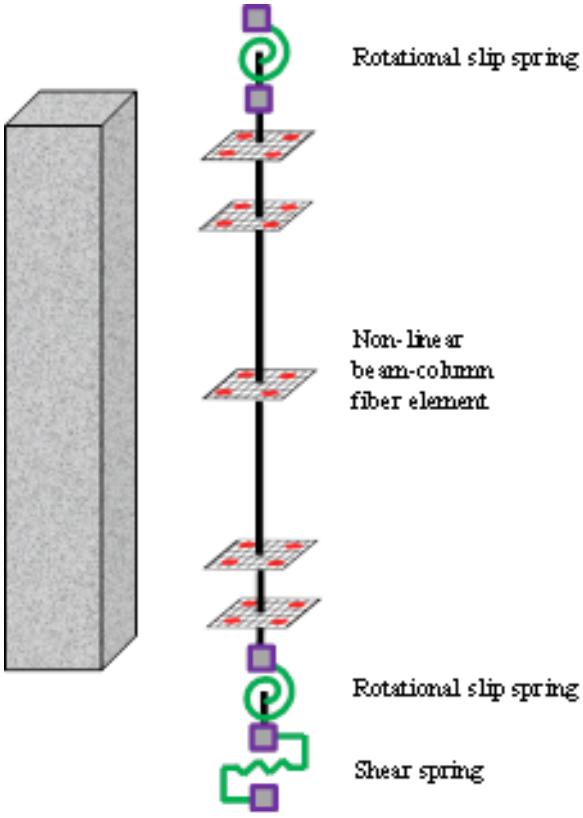

Figure 2. Numerical model adopted in this study.

the columns that are in elevation).

Finally, regarding shear deformation, in general it is admitted that in slender columns the contribution of the shear flexibility on the total displacement can be neglected: it starts to have a significant effect only on squat elements with an height-to-depth ratio lower than three. However, it becomes relevant in any case, if the element is

expected to be damaged in shear.

2.1 Flexural Response

The flexural behaviour can be modelled using a nonlinear force-based beam-column element available in OpenSEES (McKenna at al. 2000). The peculiarity of a finite element with a force formulation is that it employs linear shape functions to represent the distribution of internal generalized forces, so that that just one element is sufficient to capture the bending behaviour of the whole column, despite the fact that the formation of plastic hinges at the ends of the element will produce a concentration of curvature (far beyond the linear elastic pattern). The response of the beam-column is obtained through the integration of the responses obtained at section level, in this case a weighted summation adopting a Gauss-Lobatto scheme has been adopted over a certain number of monitored sections (for example n_s=5).

The element cross-sections have been discretized in fibres. Since a reinforced concrete element is essentially composed by two different materials: casted in place concrete and steel reinforcing bar, two different kind of constitutive relationships are used to describe the mechanical behaviour of those materials, and assigned to relevant fibres within the element sections.

The concrete has been modelled in OpenSEES using the Concrete04 uniaxial material which is based on the Popovics (Popovics 1973) law. The concrete on the section cover has been considered unconfined, whilst the concrete in the section core has been considered as confined, using the Mander et al. model. The constitutive model by Menegotto and Pinto is adopted for steel, (Steel02 uniaxial material in OpenSEES).

2.2 Slip Response

The slippage of the reinforcing bars will cause rigid-body rotation of the column, that produces an additional source of deformation, that can be significant.

Several bond slip models are available in literature for deformed bars (Eligehausen et al. 1983, Sezen and Setzler 2008, CEB-FIB Model Code 2010).

In order to account for the slippage in the numerical model, a rotational slip springs at the bottom and at the top of the column with linear constitutive relationship were used and their stiffness is given by (Elwood and Moehle 2003)

$$K_{slip} = \frac{8uEI_{eff}}{f_y \phi_{long}} \quad (1)$$

where ϕ_{long} is the diameter of longitudinal rebar, f_y is the yield strength of longitudinal rebar, u is the average tension on the surface between the longitudinal reinforcement and the concrete that can be calculated as $0.5\sqrt{f_c}$ where f_c is the concrete compressive strength and EI_{eff} is the effective stiffness that can be evaluated by (Elwood and Eberhard 2006):

$$\begin{cases} EI_{eff} = 0.2E_cI_g \quad if\ 0.2 \geq \dfrac{P}{A_g f_c} \\ EI_{eff} = E_cI_g\left(\dfrac{5}{3}\dfrac{P}{A_g f_c} - \dfrac{40}{30}\right) \quad if\ 0.2 \leq \dfrac{P}{A_g f_c} \leq 0.5 \\ EI_{eff} = 0.7E_cI_g \quad if\ 0.5 \leq \dfrac{P}{A_g f_c} \end{cases} \quad (2)$$

where P is axial load, A_g is gross area of section, E_c is the Young's module of the concrete and I_g is the section gross moment of inertia ($bh^3/12$).

2.3 Shear Response

In the past, different shear-capacity models have been proposed to account for the shear-strength degradation of columns under seismic loading. The first one was the formulation in the ATC seismic design guidelines, where a shear-capacity curve degrading with displacement ductility was proposed (Figure 3).

In this study the phenomenological model illustrated in Figure 4 has been adopted for modelling the shear spring, accounting for both strength and deformation components due to shear action.

As shown in figure 4, the branch OAB represents the backbone behaviour of the shear component of the element before the attainment of the peak of the shear strength domain (branch BC).

The pre-cracking shear stiffness $K_{S,uncracked}$ can be calculated through the elasticity theory:

$$K_{S,uncraked} = \frac{GA_v}{H} \quad (3)$$

$$G = \frac{E_c}{2(1+\nu)} \approx 0.4E_c \quad (4)$$

where: H is the column height, G, E_c and ν are respectively the shear, Young's and Poisson's modulus of concrete, and A_v is the shear effective area of the column. In general, this stiffness is contributing to a minor displacement increase, since even in squat elements where the flexural stiffness is significantly smaller, but it can be useful to modify the fiber element formulated within OpenSEES as an Euler-Bernoulli beam-

column to a full Timoshenko element.

The post-cracking shear stiffness $K_{S,cracked}$ can be calculated considering the deformation of transversal steel through the diagonal cracks. Park and Paulay (1975) proposed an equivalent strut-model:

$$K_{S,craked} = \frac{\rho_t \sin^4(\theta)\cot^2(\theta)}{\sin^4(\theta)+10\rho_t} E_s A_v \quad (5)$$

where ρ_t is the transversal steel reinforcement ratio, θ is the angle between the diagonal cracks and the member axis and E_s is the Young's modulus of steel.

The BCDE branch represent a sort of shear-strength domain representing the maximum shear force that the column can sustain. As it is evident, that limit state curve is not constant, as in the usual formulation contained in many design codes (e.g. Eurocode 2, ACI-318), but is dependant with the displacement and the element once reached the maximum strength (represented by the BC branch), will follow the degrading CD branch.

In literature there are several shear-capacity models that have been proposed to account for the shear-strength degradation of columns under seismic loading, among which (Sezen and Moehle 2004, Biskinis et al. 2004, Kowalsky and Priestley 2000, Elwood and Moehle 2005, Rasulo et al. 2002).

As shown in Figure 3, the failure is activate when the shear capacity curve (bold black dash line) intercept the shear demand curve (black line) which represent the global behaviour of the column given by the summation of the flexure, slippage and shear behaviours.

In the Sezen and Moehle model the nominal shear strength is computed as the summation of the contribution from concrete V_c and the transverse reinforcement V_s

$$V_n = V_c + V_s \quad (6)$$

where the concrete contribution can be calculated by

$$V_c = k\left(\frac{0.5\sqrt{f_c'}}{a/d}\sqrt{1+\frac{P}{0.5\sqrt{f_c'}A_g}}\right)0.8A_g\ (MPa) \quad (7)$$

while the steel contribution can be calculated by

$$V_s = k\frac{A_w f_y d}{s} \quad (8)$$

where f_c' is the compressive strength of concrete, A_g is gross area of section, P is the axial load, a is the shear span (distance between the maximum bending section and the point of inflection), d is effective depth of the section, A_w is the transversal

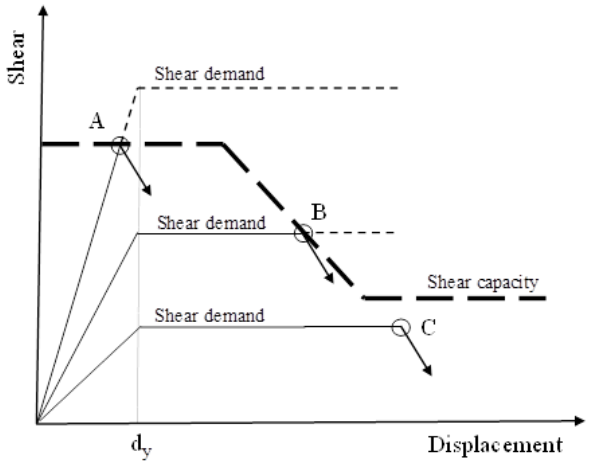

Figure 3. ATC model for shear-strength degradation. dy: yielding displacement. A: shear failure before flexural yielding (pure shear failure). B: shear failure after flexural yielding (shear-flexural failure). C: flexural failure.

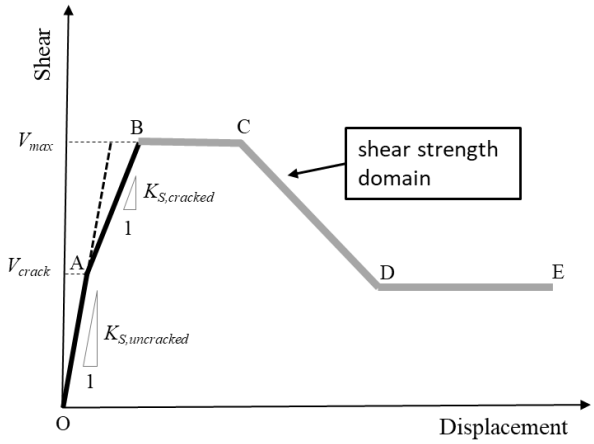

Figure 4. Phenomenological model for the shear spring

reinforcement area, f_y is the yield strength of the transversal reinforcement. The factor k is the parameter which consider the variation of shear strength with increase of displacement ductility and is defined to be equal to 1.0 for displacement ductility less than 2, to be equal to 0.7 for displacement ductility exceeding 6 and vary linearly for intermediate displacement ductility, as shown in Figure 5.

In the Biskinis et al. model the nominal shear strength is calculated as the summation of three contribution from concrete V_c , transversal reinforcement V_s and axial load V_P

$$V_n = V_c + V_s + V_P \quad (9)$$

where the concrete contribution is given by

$$V_c = k\left[0.16max(0.5;100\rho_{tot})\left(1-0.16min\left(5;\frac{a}{h}\right)\right)\sqrt{f_c}A_g\right] \quad (10)$$

the transversal reinforcement contribution is given by Equation (8), as in previous model, and the contribution of axial load is given by:

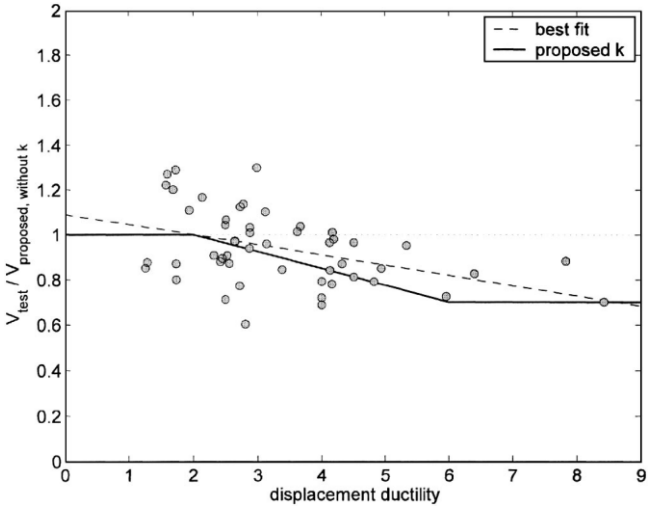

Figure 3. Factor k (Sezen and Moehle 2004)

$$V_P = \frac{h-c}{2a}\min(P; 0.55A_g f_c) \quad (11)$$

where ρ_{tot} is the total longitudinal reinforcement ratio, h is the depth of the section and c is the neutral axis deepth.

The factor k is only function of the plastic part of the displacement ductility and is given by:

$$k = 1 - 0.05 \cdot \min\left(5; \mu_\Delta^{pl}\right) \quad (12)$$

where

$$\mu_\Delta^{pl} = \frac{\Delta-\Delta_y}{\Delta_y} = \frac{\theta-\theta_y}{\theta_y} \quad (13)$$

Where Δ and θ are respectively the displacement and rotation at the point considered while Δ_y and θ_y are respectively the yielding displacement and yielding rotation.

Similar at this model is the Kowalsky and Priestley model or UCSD Modified in fact the nominal shear strength can be evaluated by the Equation (9) where the concrete contribution can be calculated by

$$V_c = \alpha\beta\gamma\sqrt{f_c}\left(0.8A_g\right) \quad (14)$$

where the α factor is function of the ratio *a/d*, the β factor is function of the longitudinal steel ratio, and the γ factor is function of the ductility curvature, as shown in Figure 6, 7 and 8.

The transversal contribution is given by

$$V_s = \frac{A_w f_y (d-c-\delta)}{s} \cdot \cot\theta \quad (15)$$

where δ is the concrete cover and s is the transverse reinforcement spacing. The axial load contribution is given by

$$V_P = P\frac{h-c}{2\,a} \;\; if\; P > 0$$
$$V_P = 0 \;\; if\; P \le 0 \quad (16)$$

Finally, the model by Elwood and Moehle introduce a drift capacity model based on observations from the experimental database, it is different than previous model because it allows to

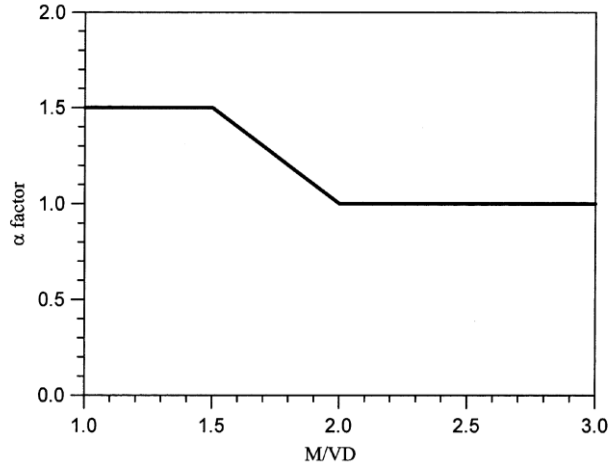

Figure 4. α factor (Kowalsky and Priestley 2000)

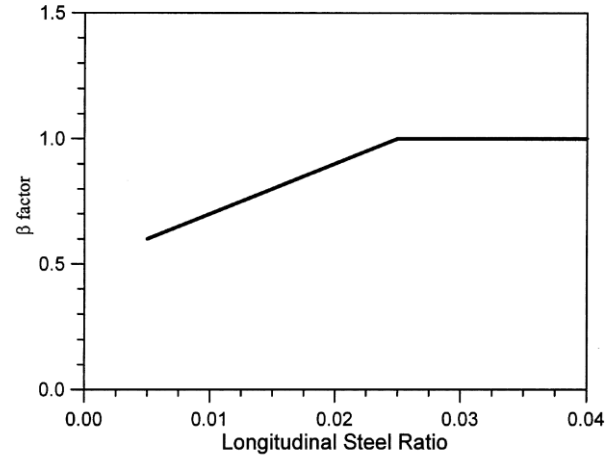

Figure 5. β factor (Kowalsky and Priestley 2000)

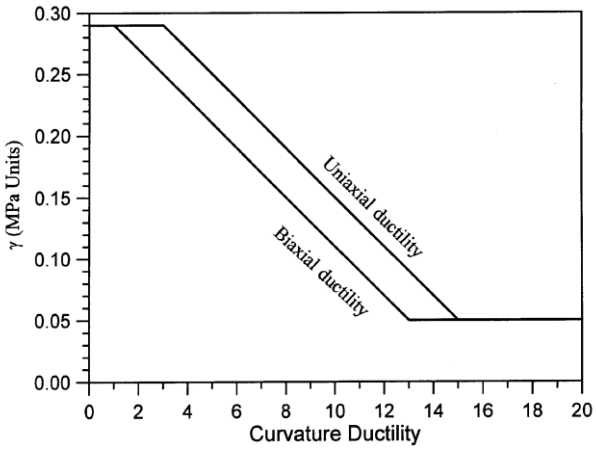

Figure 6. γ factor (Kowalsky and Priestley 2000)

evaluate the drift ratio at shear failure rather than the shear strength. The empirical equation is

$$\frac{\Delta_s}{L} = \frac{3}{100} + 4\rho'' - \frac{1}{40}\frac{\nu}{\sqrt{f_c}} - \frac{1}{40}\frac{P}{A_g f_c} \geq \frac{1}{100} \quad (MPa) \quad (17)$$

where $\frac{\Delta_s}{L}$ is the drift ratio at shear failure, ρ'' is the transverse reinforcement ratio and ν is the nominal shear stress (V_{max}/A_g).

2.4 *Interaction model*

OpenSEES introduced as interaction model the *LimitStateMaterial* command, based on Elwood works (2004), used to construct a uniaxial hysteretic material object with, among others, shear damage detection and post-damage unloading stiffness based on ductility.

This command overcomes the pitfall of a simpler shear-flexure interaction model represented by having a shear spring in series with a beam column element, as it has been depicted in Figure 2. In such a model all the shear deformation is concentrated in the shear spring whilst the flexural deformation is modelled by the beam-column element. The behaviour of the shear spring and bending beam-column element are illustrated schematically in Figure 9a and 9b, respectively.

In the simple serial model if the shear strength (the maximum of the shear spring response) is less than the bending yield strength (shear corresponding to the development of plastic hinges), the total response is correctly dominated by a brittle failure occurring in the elastic branch: this is the case of the solid lines in Figure 9: the total response accounting for the flexure-shear interaction is depicted in Figure 9c.

If, on the other hand, the shear strength is higher than the bending yield strength (as illustrated by the dash-lines in Figure 9), then the model is not able to capture any shear degradation, in contrast with theoretical and experimental evidences.

Indeed, in the latter case, when the initial shear strength is higher than yielding strength, but close enough to it that when degrading with the increase of inelastic deformation would at some point become lower, we expect the activation of a shear damage phenomenon in the plastic branch, as shown in Figure 3b, that leads the structural response of the column to follow the degrading CDE branch of the shear-strength-domain of Figure 4.

In order to improve the series model, the *LimitStateMaterial* associated with *LimitCurve* command can be used to define a limit shear surface defined by the drift capacity model proposed by Elwood, with the use of the shear-failure domain given by Equation (17).

Adopting the Elwood model, prior of the activation of the degrading branch the response will follow the behaviour given by the summation of flexure, shear and slippage (as in the simple serial spring model). After each step the Limit

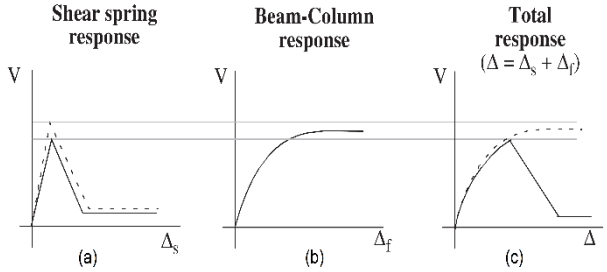

Figure 7. Shear spring in series model (Elwood 2004)

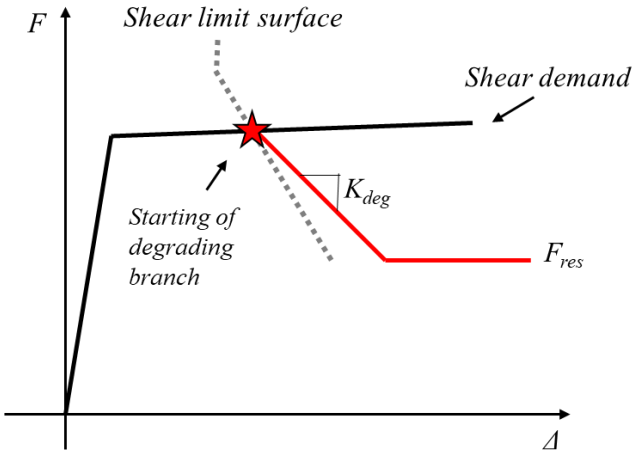

Figure 8. Redefinition of backbone after failure

Curve model checks if the force and deformation have exceeded the limit surface. If the limit curve has not been exceeded the analysis continue at the next step without any change to the behaviour. If the limit curve has been exceed, then the behaviour is redefined according to the degrading slope K_{deg}, and residual strength F_{res}, (Figure 10).

3 NUMERICAL VALIDATION

Using the model illustrated in the previous chapter, the experimental behaviour of a series of full-scale columns tested by Lynn 2001 was simulated analytically by OpenSEES (Grande and Rasulo 2013, Grande and Rasulo 2015, Rasulo et al. 2019). Lynn tested a set of 8 columns.

The columns had a double cantilever configuration, a square cross-section of 457 x 457 mm. The longitudinal steel reinforcement was placed uniformly around the perimeter of the cross-section and they were 32 mm (#10) as nominal diameter. The transversal reinforcements were hoop with 9.5 mm (#3) and 457 mm respectively as nominal diameter and spacing (ρ"=0.001). The axial force was equal to $P = 503$ kN. The concrete compressive strength was equal to $f_c = 26$ MPa, whilst the longitudinal steel yielding strength was equal to $f_{yl} = 335$ MPa and

the transversal steel yielding strength was equal to f_{yw} = *400 MPa*.

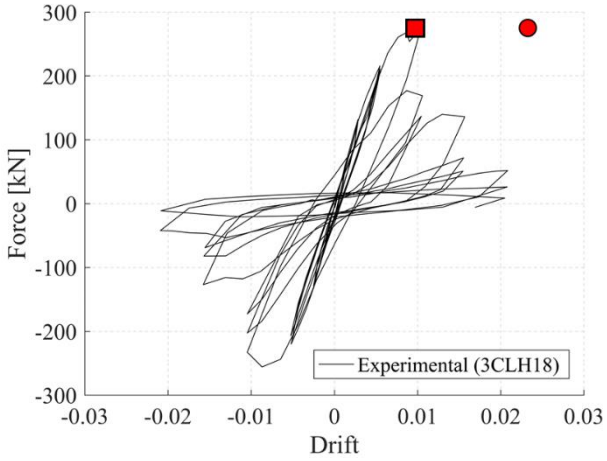

Figure 9. Experimental behaviour. The square and circle marks represent experimental and calculated (Elwood, 2004) initiation of shear dedradation.

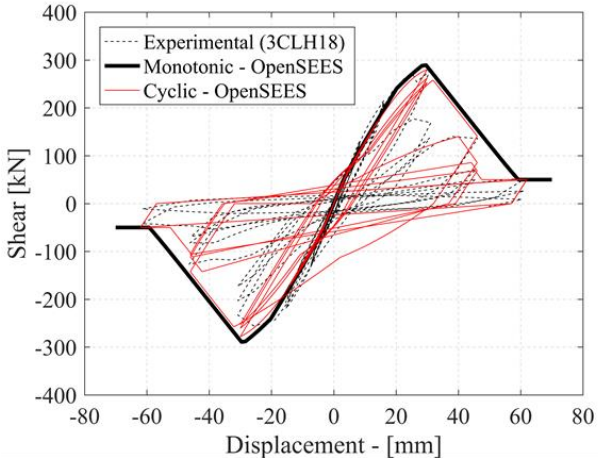

Figure 10. Comparison of numerical cyclic response with experimental results after the calibration of some parameters

In the numerical model the stiffness of the AB branch employed has been set equal to the one of the previous branch (OA), following, therefore, the black dash line of Figure 3.

In Figure 11 the experimental behaviour of the 3CLH18 specimen is shown.

Experimental behaviour shows clearly a shear strength degradation in plastic branch due at shear failure immediately after flexural yielding.

It is clearly from the experimental curve that the shear degradation starts at a drift value of about $(\Delta_s/L)_{exp}$=0.01 and displacement of about $\Delta_{s,expt}$=30.4 mm (square mark in Figure 11).

Using Equation (17) is possible to calculate the drift ratio and displacement at shear degradation that are $(\Delta_s/L)_{calc}$=0.024 and $\Delta_{s,calc}$ =71.4 mm, respectively (circle mark in Figure 11).

From the comparison between the experimental and calculate results is clear that the drift capacity model of Elwood, in this case, gives a value much higher in term of drift ratio and displacement at shear failure than the one experienced experimentally.

Since the Limit Curve model is based on this empirical equation to define the shear limit surface theoretically it could not work correctly. Therefore we recalibrated equation 17 in order to better approximate with OpenSEES the experimental curve, as shown in Figure 12 where the black line is the numerical monotonic behaviour and the red line is the cyclic one.

4 CONCLUSION

The present study is focused on the modelling with OpenSEES of RC column subject to complex phenomena of flexure-shear interaction.

The Limit State Material, after the calibration of some parameters, was able to approach correctly the experimental behaviour.

However, it should be recognized that the series model shows in Figure 2 is not able to account the localized deformations over the height of the column but is able only to approach the global behaviour of the column.

REFERENCES

ACI 318. 2019. Building Code Requirements for Structural Concrete and Commentary (ACI 318-19), American Concrete Institute. Farmington Hills, MI, 48331-3439 USA

Biskinis, D.E., Roupakias, G.K., Fardis, M.N., 2004. Degradation of Shear Strength of Reinforced Concrete Members with Inelastic Cyclic Displacements, *ACI Structural Journal*, **101**(6), 773-783.

Calvi, GM., Pavese, A., Rasulo, A., 2000. Experimental Studies of the Response of Hollow Bridge Piers, *Implications of recent earthquake on seismic risk.*

Calvi, GM, Pavese A., Rasulo, A., Bolognini, D., 2005. Experimental and numerical studies on the seismic response of R.C. hollow bridge piers, *Bulletin of Earthquake Engineering*, **3**(3), 267-297.

CEB-FIB Model Code 2010-Final draft, 2010. Thomas Telford, Lausanne, Switzarland.

Di Ludovico, M., Digrisolo, A., Graziotti, F., Moroni, C., Baltzopoulos, G., Biondi, S., Borri, A., Caprili, S., Carocci, C., Dall'Asta, A., Dezi, L., De Santis, S., Di Fabio, F., Di Sarno, L., Ferracuti, B., Ferretti, D., Fiorentino, G., Ianniruberto, U., Mannella, A., Mazzotti, C., Podestà, S., Riva, P., Sandoli, A., Silvestri, S., Sorrentino, L., Vignoli, A., Magenes, G., Masi, A., Prota, A., Dolce, M., Manfredi, G., 2017. The contribution of ReLUIS to the usability assessment of school buildings following the 2016 Central Italy earthquake, *Bollettino di Geofisica Teorica ed Applicata*, **58**(4), 353-376.

Eligehausen, R., Bertero, V.V., Popov, E. P., 1983. Local bond stress-slip relationships of deformed bars under

generalized excitations: Tests and analytical model, *Earthquake Engineering Research Center*, Univ. of California, Berkeley, Calif., Report No EERC, 83-23.

Elwood, K.J., Moehle, J.P., 2003. Shake Table Tests and Analytical Studies on the Gravity Load Collapse of Reinforced Concrete Frames, *PEER Pacific Earthquake Engineering Research Center*, **2003/01**.

Elwood, K.J., 2004. Modelling failures in existing reinforced concrete columns, *Canadian Journal of Civil Engineering*, **31**(5), 846-859.

Elwood, K.J., Moehle J.P., 2005. Drift Capacity of Reinforced Concrete Columns with Light Transverse Reinforcement, *Earthquake Spectra*, **21**(1), 71-89.

Elwood, K.J., Eberhard, M.O., 2006. Effective Stiffness of Reinforced Concrete Columns, Research Digest No 2006-1, *PEER Pacific Earthquake Engineering Research Center*.

Eurocode 2, 2004. Design of concrete structures - Part 1-1: General rules and rules for buildings (EN 1992-1-1). European Committee for Standardization. Bruxelles.

Forte, A., Santini, S., Fiorentino, G., Lavorato, D., Bergami, A.V., Nuti, C., 2018. Influence of Materials Knowledge Level on the Assessment of the Shear Strength characteristic Value of Existing RC Beams. In *Proceedings of the 12th fib International PhD Symposium in Civil Engineering*, Bily P.,Kohoutkova A., Vitek J.L., Frantova, M., Eds, Czech Technical University, pp 979-986.

Grande, E., Rasulo, A., 2013. Seismic assessment of concentric X-braced steel frames, *Engineering Structures*, **49**, 983-995.

Grande, E., Rasulo, A., 2015. A simple approach for seismic retrofit of low-rise concentric X-braced steel frames, *Journal of Constrctional Steel Research*, **107**, 162-172.

Imperatore, S., Lavorato, D., Nuti, C., Santini, S., Sguerri, L., 2012. Numerical Modeling of Existing RC Beams Strengthened in Shear with FRP U-Sheets, In *Proceedings of the 6th International Conference on FRP Composites in Civil Engineering*, CICE 2012, International Institute for FRP in Construction (IIFC).

Imperatore, S., Lavorato, D., Nuti, C., Santini, S., Sguerri, L., 2013. Shear Behavior of Existing RC T-Beams Strengthened with CFRP. In Assessment, Upgreding and Refurbishment of Infrastructures, *International Association for Bridge and Structural Engineering (IABSE).*

Kowalsky, M.J., Priestley M.J.N., 2000. Improved Analytical Model for Shear Strength of Circular Reinforced Concrete Columns in Seismic Regions, *ACI Structural Journal*, **97**(3), 388-396.

Lavorato, D., Bergami, A. V., Nuti, C., Briseghella, B., Xue, J., Tarantino, A.M., Marano, G.C., Santini, S., 2017. Ultra-High-Performance Fibre-Reinforced Concrete Jacket for the Repair and the Seismic Retrofitting of Italian and Chinese RC Bridges, *COMPDYN 2017-Proceedings of the 6th International Conference on Computational Methods in Structural Dynamics and Earthquake Engineering*, M. Papadrakakis, M. Fragiadakis (eds.), National Technical University of Athens, **1,** 2149-2160.

Lavorato, D., Nuti, C., Santini, S., 2018a. Experimental Investigation of the Shear Strength of RC Beams Extracted from an Old Structure and Strengthened by Carbon FRP U-Strips, *Applied Science (Switzerland)*, **8**(7).

Lavorato, D., Bergami, A.V., Fiorentino, G., Fiore, A., Santini. S., Nuti, C., 2018b. Experimental Tests on Existing RC Beams Strengthened in Flexure and Retrofitted for Shear by C-FRP in Presence of Negative Moments, *International Journal of Advanced Structural Engineering* , **10**(3), 211-232.

Lavorato, D., Pelle, A., Fiorentino, G., Nuti, C., Rasulo, A., 2019. A nonlinear material model of corroded rebars for seismic response of bridges, *COMPDYN 2019, 7th ECOMAS Thematic Conference on Computational Methods in Structural Dynamics and Earthquake Engineering*, M. Papadrakakis, M. Fragiadakis (eds.), Crete Island, Grecee, 24-26 June 2019.

Lynn, A., 2001. Seismic Evaluation of Existing Reinforced Concrete Building Column, PhD Dissertation, University of California at Berkeley.

Marino, E.M., Barbagallo, F., Angiolilli, M., Belletti, B., Camata, G., Dellapina, C., Di Domenico, M., Fiorentino, G., Gregori, A., Lavorato, D., Lima, C., Martinelli, E., Rasulo, A., Ricci, P., Ruggieri, S., Spacone, E., Terrenzi, M., Uva, G., Verderame, G., 2019. Influence of Nonlinear Modeling on Capacity Assessment of RC Framed Structures, *COMPDYN 2019, 7th ECOMAS Thematic Conference on Computational Methods in Structural Dynamics and Earthquake Engineering*, M. Papadrakakis, M. Fragiadakis (eds.), Crete Island, Grecee, 24-26 June 2019.

McKenna, F., Fenves, G.L., Scott, M.H., Jeremic, B., 2000. Open System for earthquake engineering simulation (OpenSEES), Univ. of California, Berkeley, CA. http://OpenSEES.berkeley.edu.

Park, R., Paulay, T. 1975. *Reinforced concrete structures*. John Wiley & Sons.

Popovics, S., 1973. A numerical approach to the complete stress-strain curve of concrete, *Cement and concrete research*, **3**(5), 583-599.

Rasulo, A., Testa, C., Borzi, B., 2015. Seismic risk analysis at urban scale in Italy, *Lecture Notes in Computer Science*, **9157**, 403-414.

Rasulo, A., Fortuna, M.A., Borzi, B., 2016. Seismic risk analysis at urban scale in Italy, *Lecture Notes in Computer Science*, **9788**, 198-213.

Rasulo, A., Pelle, A., Lavorato, D., Fiorentino, G., Nuti, C., 2019. Flexure-Shear interaction in seismic assessment of reinforced concrete buildings, Proceedings of Opensees Days Eurasia, First Eurasian Conference on Opensees, 20-21 June, 2019, Hong Kong.

Sezen, H., Moehle J.P., 2004. Shear Strength Model for Lightly Reinforced Concrete Columns, *Journal of Structural Engineering*, **130**(11), 1692-1703.

Sezen, H., Setzler, E.J., 2008. Reinforcement slip in reinforced concrete columns, *ACI Structural Journal*, **105**(3), 280.

Zhou, Z, Nuti, C., Lavorato, D., 2014. Modeling of the Mechanical Behaviour of Stainless Reinforcing Steel, In *Proceedings of the 10th fib International PhD Symposium in Civil Engineering*, Rouleau N., Bastien J., Fiset M., Thomassin M, Eds, Universite Laval, 515-520.

Zhou, Z., Lavorato, D., Nuti, C., Marano, G.C., 2015. A model for carbon and stainless steel reinforcing bars including inelastic buckling for evaluation of capacity of existing structures, *COMPDYN 2015 – 5th ECOMAS Thematic Conference on Computational Methods in Structural Dynamics and Earthquake Engineering*, 876-886.